

Research on the detection performance of infrared photoelectric tracking system for high-speed projectile

XIAOQIAN ZHANG*

School of Electronic and Information Engineering, Xi'an Technological University, Xi'an 710021, China

In order to evaluate the detection performance of the infrared photoelectric tracking system for high-speed projectile and establish a stable target tracking platform, the projectile radiation characteristics of the detection area of the infrared photoelectric tracking system based on the imaging detection principle is studied, the projectile reflection radiation model and the projectile infrared radiation model are established, and the calculation function of the projectile total radiation intensity is given. Combining the inherent parameters of the system, the calculation model of detection distance of the system is constructed, and the detection performance of the system is analyzed. Based on the design parameters of the infrared photoelectric tracking system, the variation rules of radiation energy obtained from the sensitive surface of the infrared imaging sensor under the sky background brightness, different flying attitudes of the projectile and different detection distances are calculated and analyzed; the correctness and scientificity of the detection distance model of the infrared photoelectric tracking system is verified by collecting the information of the system output target signal under different test conditions.

(Received March 14, 2023; accepted August 7, 2023)

Keywords: Infrared photoelectric tracking system, Infrared radiation, Signal-to-noise ratio, Detection distance

1. Introduction

The infrared photoelectric tracking system has the advantages of all-weather operation and strong anti-interference ability, and is widely used in military reconnaissance, precision guide weapon, intelligent navigation systems, human-computer interaction and other fields. Obtaining the relevant information of high-speed projectile targets in the complex environment is an important task for testing and evaluating weapon equipment in the shooting range. The infrared photoelectric tracking system is used to detect the high-speed projectile target information of the external ballistics in the shooting range, and track the infrared target in real time and reliably. Infrared target tracking, as a branch of target tracking technology, has many similarities with color target tracking: both require extracting the appearance features of the target from the image and using them as templates for subsequent frame tracking. Most infrared target tracking algorithms are based on traditional non deep learning. Yang et al. [1] proposed an infrared target tracking algorithm based on sparse encoded histogram features and disturbance perception models, which effectively removes background interference by utilizing the structural characteristics of infrared targets. Zhao et al. [2] used image guided filtering and kernel correlation filtering methods to effectively distinguish background edges and track small infrared targets. In recent years, deep learning algorithm has been widely used in the field of target tracking. Researchers have applied convolutional neural network to infrared target tracking to improve the algorithm performance. Tang et al. [3-4] proposed a decision level fusion detection

and tracking method for infrared and visible light based on deep learning, which extracts color target models from existing depth models to train infrared tracking algorithms. The MCFTS algorithm integrates multi-layer features of the VGG-Net neural network, achieving optimization in feature extraction and constructing an overall thermal infrared tracker. However, the optimization of features greatly reduces the speed of the tracker [5]. As a data-driven method, deep learning can learn potential rules and trends that are difficult to express by explicit models from big data. Therefore, many scholars have applied it to target tracking, using neural networks to learn knowledge about the target and environment to improve the performance of classic algorithms, forming a hybrid driven target tracking algorithm with data and model. The research on hybrid driven target tracking mainly focuses on estimating and modifying the motion model parameters, intermediate parameters, and estimated output of classical model driven algorithms, which has improved the tracking performance of classical tracking algorithms to a certain extent [6-7]. In the infrared photoelectric tracking system, the detection ability of the system restricts the accuracy and reliability of the tracking flying target [8]. In addition, for users, the detection ability of the system is also a very important parameter. The calculation of the detection distance of the system is a very complex problem, it is determined by the parameters related to the target, background, atmospheric transmission, imaging sensor, readout circuit and image processing algorithm, and it is particularly important to master the impact of these parameters on the system performance index. For the infrared photoelectric tracking system, the main factors affecting its performance include the detection

performance of imaging sensor, optical lens parameters, optical lens transmittance and the radiation energy of the flying projectile itself; At the same time, due to the complexity of the detection environment of the system, the change of the sky background brightness, the size of the projectile, the detection distance and other factors have a great impact on the detection performance of the system. Many scholars and researchers at home and abroad have conducted in-depth research on the technical parameters of the infrared optical system, and proposed the operating range model respectively [9-11]. For the research on the detection distance of infrared photoelectric system, in response to the limitations and imperfections of the distance equation in traditional infrared systems, Cao et al. [12] established the operating range equation of infrared system for point source target and area source target in combination with the factors of background radiation intensity, target imaging dispersion and imaging effect, and they were tested and validated using typical target outfield experimental data; Mu and Han [13] established a detection distance model based on noise equivalent temperature difference (NETD), which is applicable to the evaluation of detection performance of staring infrared imaging system; NETD is the ideal value measured in the laboratory, without considering the actual situation of the test environment; Mao et al. [14] proposed a detection distance model based on noise equivalent flux density (NEFD), but the model also did not consider the dispersion characteristics of target imaging. Research workers have conducted modeling and application research on ground-based infrared measurement system for the operating range of air targets [15-16]; the detection ability of airborne infrared measurement system is analyzed and studied in reference [17]. In addition, in references [18-20], the movement characteristics and infrared radiation

characteristics of the projectile target are studied, and the calculation function of the radiant energy of the projectile surface is established; and using computer simulation of flying trajectory curves and the variation curve of flying surface temperature with time, the variation curve of target radiance with time under given conditions was obtained, and the characteristics of the projectile target that met the experimental measurement requirements were obtained; However, the influence of environmental illumination changes on the optical characteristics of projectiles and the radiation energy of flying projectiles has not been reported in detail. In foreign countries, foreign researchers have carried out some basic discussions and studies on the detection ability of infrared photoelectric system, mainly focusing on imaging sensor, but there is relatively little research on environmental impact. In order to improve the detection ability of the infrared photoelectric tracking system, the paper mainly starts from the radiometry and photometry, combines the infrared photoelectric tracking and detection principle, establishes the target radiant energy calculation model and detection range calculation model of the system, and verifies the scientificity of the established detection distance model based on the tracking platform.

2. Optical detection principle of infrared photoelectric tracking system

Fig. 1 is the optical detection principle of the infrared photoelectric tracking system, which is mainly composed of the infrared optical detection module, the signal processing module, the acquisition module and the processing computer.

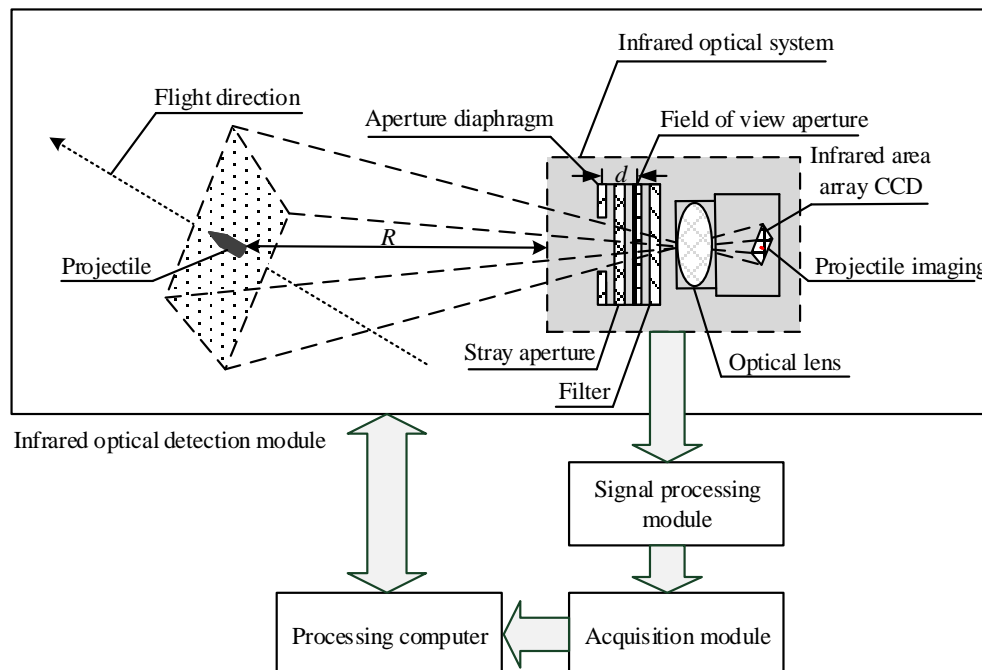


Fig. 1. Optical detection principle of infrared photoelectric tracking system

In Fig. 1, the infrared optical detection module is equipped with an aperture diaphragm, a stray aperture, a field of view aperture, a filter and an infrared imaging sensor (infrared area array CCD). The internal structure of the dashed frame in Fig. 1 is an infrared optical system. When the projectile passes through the detection field of the detection area, the radiation energy generated by the projectile's surface enters the photosensitive surface of the infrared area array CCD through the field aperture and aperture diaphragm; then, the infrared area array CCD output the radiation energy of the flying projectile after the signal processing module; next, the target information detected by the system through the acquisition module is displayed directly in the processing computer; finally, the processing computer monitors the detection status of flying projectiles by the infrared optical detection module through wireless communication, so as to realize the system's reliable tracking effect, because stable detection performance is the premise of locating and tracking the flying projectile. In the infrared photoelectric tracking system, the distance between the field of view aperture and the aperture diaphragm is d , and the clutter elimination aperture is added in the field of view aperture and the aperture diaphragm. The purpose is to suppress the interference of environment brightness. At the same time, in order to eliminate the impact of strong background brightness on the detection optical system, a filter is added at the front end of the field of view aperture. The distance between the flight projectile and the optical detection system is R . At this distance, the red area represents the imaging size of the projectile in the infrared area array CCD.

3. Modeling of projectile radiation characteristics

3.1. Projectile reflection radiation modeling

In the process of detecting high-speed projectile by infrared photoelectric tracking system, due to the close

$$I_{s-e} = \frac{\rho_{tr}}{\pi} \int_{\lambda_1}^{\lambda_2} [E_{sun}(\lambda) \cos \theta_{st} A_{st} + E_{earth}(\lambda) \cos \theta_{et} A_{et}] \cdot \cos \beta_{id} d\lambda \quad (3)$$

In formula (3), ρ_{tr} is projectile's surface reflectance, and β_{id} is the included angle between reflected radiation direction and normal direction of projectile's surface.

3.2. Projectile infrared radiation modeling

The projectiles fly in the air at multiple speed of sound, and they generate high-speed friction with the gas in the atmosphere, heating the projectile's surface to increase its surface temperature, reflecting the different infrared radiation characteristics of projectiles. Considering the projectile as a gray body, according to the blackbody radiation law [21], the radiation brightness of the projectile's surface is:

distance between the system and the projectile, this paper does not consider the radiation effect of atmospheric and cloud radiation sources in the environment, but only considers the radiation of the sun and the surface, the two radiation sources act on the projectile's surface at different incident angles.

During the flying process of high-speed projectile, the projectile itself is not luminous. If the solar spectral irradiance is $E_{sun}(\lambda)$ and the wave band of the imaging sensor is $\lambda_1 \sim \lambda_2$, the irradiance generated by the solar radiation on the surface of the projectile in the detection area is:

$$E_{st} = \int_{\lambda_1}^{\lambda_2} E_{sun}(\lambda) \cos \theta_{st} A_{st} d\lambda \quad (1)$$

In formula (1), λ_1 and λ_2 are the spectral wavelengths corresponding to the photoelectric detector, θ_{st} is the included angle between the incident direction of solar radiation and the normal direction of the projectile's surface, and A_{st} is the radiation area from the sun to the projectile's surface.

In addition to the solar spectrum acting on the projectile's surface, the surface radiation also acts on the projectile's surface. Assuming that the spectral irradiance of the surface is $E_{earth}(\lambda)$, and the included angle between the incident direction of the terrestrial radiation and the normal direction of the projectile's surface is θ_{et} , the irradiance generated by the direct surface radiation on the projectile's surface is:

$$E_{et} = \int_{\lambda_1}^{\lambda_2} E_{earth}(\lambda) \cos \theta_{et} A_{et} d\lambda \quad (2)$$

In formula (2), A_{et} is the radiation area from the surface radiation to the projectile's surface.

The irradiance generated by the direct radiation of the sun and the surface on the projectile's surface is reflected and the reflected radiation intensity is:

$$L_t = \frac{\rho_{tr}}{\pi} \int_{\lambda_1}^{\lambda_2} \frac{c_1}{\lambda^5 (e^{c_2/\lambda T_t} - 1)} d\lambda \quad (4)$$

In formula (4), c_1 is the first radiation constant, c_2 is the second radiation constant, and T_t is the projectile's surface temperature, this temperature is caused by the friction between the projectile's surface and the air when the projectile is flying at high speed. It can be obtained according to the detection ambient temperature and the flying speed of the projectile, and is expressed by formula (5).

$$T_t = T_e (1 + 0.164M^2) \quad (5)$$

In formula (5), T_e is the detection ambient temperature, and M is the Mach number corresponding to the flying speed of the projectile [22]. At the same time, the change of the projectile's surface temperature in high-speed flying process is also affected by the insulating wall temperature. If the flying speed of the projectile at a specific time is known, according to formula (5), the insulating wall temperature can be obtained as:

$$T_{tw} = T_e (1 + \sqrt{P_r} 0.164M^2) \quad (6)$$

In formula (6), $\sqrt{P_r}$ is Prandtl Number. During the high-speed flying of the projectile in the air, the heat flow direction between the projectile's surface and the air current depends on the relationship between the projectile's surface temperature and the insulating wall temperature. When the projectile's surface temperature is greater than the insulating wall temperature, the heat is transferred to the gas; conversely, heat is transferred to the projectile's surface. At the same time, due to the effect of

$$\begin{aligned} I_{total} &= I_{s-e} + I_t \\ &= \frac{\rho_{tr}}{\pi} \int_{\lambda_1}^{\lambda_2} [E_{sun}(\lambda) \cos \theta_{st} A_{st} + E_{earth}(\lambda) \cos \theta_{et} A_{et}] \cdot \cos \beta_{td} d\lambda + \frac{\rho_{tr} A_t \cos \alpha_t}{\pi} \int_{\lambda_1}^{\lambda_2} \frac{c_1}{\lambda^5 (e^{c_2/\lambda T_e (1+0.164M^2)} - 1)} d\lambda \end{aligned} \quad (8)$$

4. Modeling of detection ability of the system

Based on the above calculation model of the reflected radiation characteristics of the projectile and the infrared radiation characteristics of the projectile itself, the radiation intensity of the projectile in the imaging sensor band under the environment is calculated. Assuming that R_{to} is the distance between the projectile and the imaging sensor, and combining with formula (8), the radiant flux on the imaging sensor that enters the pupil of the imaging sensor and reaches the system is:

$$\Phi_t = \int_{\lambda_1}^{\lambda_2} \frac{\tau_a \tau_o A_d}{R_{to}^2} \cdot I_{total} d\lambda \quad (9)$$

In formula (9), τ_a is the atmospheric spectral transmittance of the environment, τ_o is the spectral transmittance of the imaging sensor, and A_d is the pupil area.

Assuming that L_b is the background spectral radiance, the radiant flux of the background radiation on the imaging sensor is calculated as:

$$\Phi_b = \int_{\lambda_1}^{\lambda_2} L_b \tau_o A_d \Omega d\lambda \quad (10)$$

In formula (10), Ω is the solid angle of the optical system pupil area to the center of the flying projectile.

gravity and atmospheric drag during the flight of the projectile, the flying speed of the projectile changes in a near parabolic state, which changes the heat flow direction between the projectile's surface and the air current, reflecting the relationship between the temperature distribution of the projectile's surface and time.

Assuming that α_t is the included angle between the detection line of sight of the system and the normal direction of the projectile's surface, and A_t is the infrared radiation area of the projectile's surface; according to formulas (5) and (6), the radiation intensity of the projectile along the detection line of sight of the system is obtained as follows:

$$I_t = \frac{\rho_{tr} A_t \cos \alpha_t}{\pi} \int_{\lambda_1}^{\lambda_2} \frac{c_1}{\lambda^5 (e^{c_2/\lambda T_e (1+0.164M^2)} - 1)} d\lambda \quad (7)$$

Combining formulas (3) and (7), the total radiation intensity of the projectile's surface is obtained as follows:

In order to intuitively analyze the imaging information of the projectile on the imaging sensor, the signal processing module of the system is used to convert the radiant flux of the projectile on the imaging sensor into electrical signal information, which is:

$$Q = \kappa \cdot k \cdot (\Phi_t + \Phi_b) \cdot R_0 \quad (11)$$

In formula (11), κ is the gain of the amplification processing circuit, k is the conversion coefficient of the imaging sensor, and R_0 is the input impedance of the detection circuit.

The detection ability of the infrared photoelectric tracking system to the flying projectile can be described by the detection distance. The detection distance of the system is related to the radiation intensity of the projectile, the atmospheric spectral transmittance, the spectral transmittance of the optical system, the system equivalent noise bandwidth, the optical system aperture, the detector unit area and the signal-to-noise ratio of the system. Among, the signal-to-noise ratio of the system is described by the number of electrons generated by the projectile and background radiation on a single pixel of the imaging sensor [23], which are respectively represented as:

$$N_t = \xi \frac{\Phi_t t (\lambda_1 + \lambda_2)}{2hc} \quad (12)$$

$$N_b = \xi \frac{\Phi_b t (\lambda_1 + \lambda_2)}{2hc} \quad (13)$$

In formulas (12) and (13), ξ is the quantum conversion efficiency, t is the integral time, h is the Planck constant, and c is the speed of light.

The number of noise electrons only considers shot noise n_s and readout noise n_r in the infrared photoelectric tracking system, the readout noise is introduced by the circuit of the imaging sensor. Among, shot noise includes photon noise generated by projectile and background radiation, and dark current noise caused by thermal motion of charge carriers [24], whose expression is:

$$n_s = \sqrt{N_t + N_b + N_d} \quad (14)$$

In formula (14), N_d is the dark current noise, and

$N_d = \frac{I_d \cdot t}{q}$, where, I_d is the dark current intensity, q is the amount of electronic charge.

According to formulas (12), (13) and (14), the calculation model of signal-to-noise ratio of the system is established, which is:

$$SNR = \frac{N_t - N_b}{\sqrt{N_t + N_b + N_d + n_r^2}} \quad (15)$$

According to the influence factors of the detection ability of the system, the calculation expression of the detection distance of the infrared photoelectric tracking system is obtained.

$$R = \sqrt{\frac{I_{total} \cdot \tau_a \tau_o A_d D^*}{(\Delta f A_1)^{1/2} \cdot SNR}} \quad (16)$$

In formula (16), D^* is the average detection rate of the imaging sensor, Δf is the equivalent noise bandwidth of the system, and A_1 is the detector unit area.

5. Calculation and experimental analysis

5.1. Calculation analysis

Based on the size of the research target in this paper, the field of view angle of the optical lens can be determined by selecting the focal length of the optical lens, the size of the infrared CCD, and the farthest detection distance the system. At the same time, using an infrared CCD with the same size photosensitive surface, the higher the resolution, the better the detection performance of the

system; The resolution and size of infrared CCD, as well as the field of view angle of optical lens, are related to the detection distance of the system. In this study, it is assumed that the focal length of the selected optical lens is 125 mm, its transmittance is 0.75, and the relative aperture is 1:2.8. The photosensitive surface of the infrared imaging sensor (CCD) is 12 mm × 20 mm, its conversion response rate is $3.5 \times 10^{-6} \mu s$, and the wave band is 3 μm ~ 5 μm, the mass of the projectile is 1.2 kg, its diameter is 57 mm, and its length is 0.35 m. If the initial temperature of the projectile is 300 K, and the detection ambient temperature is 290 K, according to formula (5), when the initial speeds of the projectile are 600 m/s, 800 m/s, 1000 m/s and 1200 m/s respectively, the impact of the different initial speeds of projectile on the projectile's surface temperature is calculated, as shown in Fig. 2.

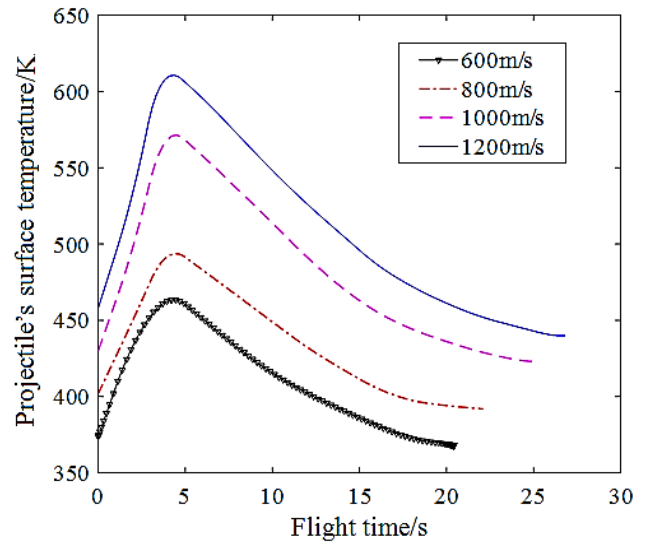


Fig. 2. Distribution of projectile's surface temperature under different initial speeds of projectile (color online)

According to Fig. 2, when the initial speed of the projectile is 600 m/s, the flying time of the projectile is 20s. During the whole flight process, the initial temperature of the projectile's surface is about 374 K, and then gradually increases. When the flying time reaches 4s, the peak of projectile's surface temperature appears, and the maximum temperature reaches 469 K. As the projectile continues to fly, the projectile's surface temperature gradually decreases, which reflects that when the projectile is out of the chamber, because the projectile is moving at high-speed in the gun chamber, the projectile and the gun itself generate friction. When the projectile is out of the chamber, its surface friction with the air, making the projectile's surface temperature continuously increase. After the flying time reaches 8s, as the flying speed of the projectile decreases gradually, the thermal energy generated by its friction with the air decreases, the projectile's surface temperature gradually decreases and tends to be stable, the results reflecting the role of the heat flow direction between the projectile's surface and the air

current. At the same time, for different initial speeds of projectile, the initial speed is the higher, the projectile's surface temperature is the greater.

When the initial speed of the projectile is 1200 m/s

and the projectile acts on the detection area at different incident angles, the relation of the radiation intensity of the projectile's surface and the wavelength is calculated according to formula (8), as shown in Fig. 3.

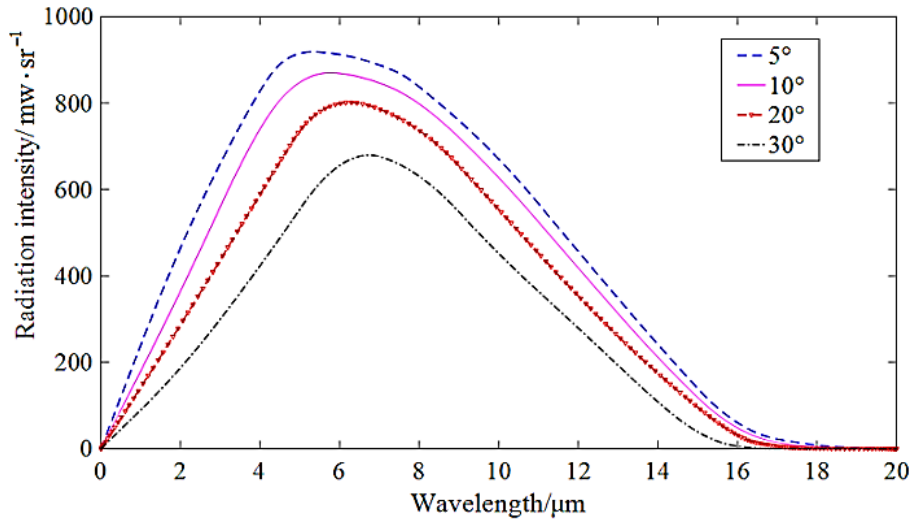


Fig. 3. Curve of radiation intensity of projectile's surface changing with wavelength (color online)

From the change curve shown in Fig. 3, the greater the incident angle of projectile, the lower the projectile's surface temperature, the results indicating that the projectile acts on the detection area with a certain incident angle, making the radiation intensity of the projectile's surface have a cosine coefficient relationship, based on this incident angle, the radiation intensity of the projectile's surface is $I'_{\text{total}} = I_{\text{total}} \cdot \cos \gamma$, γ is the incident angle of projectile. At this time, the peak wavelength of radiation intensity of the projectile's surface moves between 4 μm ~ 7 μm , and the detection rate peak wavelength of the infrared imaging sensor should also be near this band, combined with the characteristics of the response band of the infrared imaging sensor, it is not symmetrical on both sides with the response peak wavelength as the center, but shifts to the short wavelength direction, and the response rate decreases slowly in the short wavelength direction. Therefore, it is appropriate to select the infrared imaging sensor with band of 3 μm ~ 5 μm as the detector.

According to formula (16), assuming that the signal-to-noise ratio of the system is 20, and the same type of projectile at different detection distances, the radiation energy of the projectile obtained by the infrared imaging sensor is converted into the change curve of electrical signal information, as shown in Fig. 4.

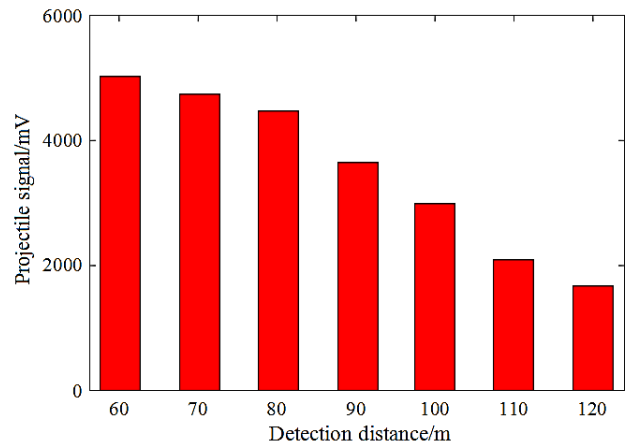


Fig. 4. Change curve of projectile signal and detection distance

It can be seen from Fig. 4 that the farther the detection distance, the less the radiation energy of the projectile obtained by the infrared imaging sensor of the system, and the smaller the amplitude of the projectile signal output by the system. According to formula (16), under certain signal-to-noise ratio conditions, the infrared photoelectric tracking system is not only related to the luminous area and spectral transmittance of the optical lens, but also related to the effective detection area of the infrared imaging sensor; When the parameters of the optical system are determined, the detection distance has an exponential relationship with the radiant energy of the projectile. In order to improve the tracking performance of the system, it is necessary to increase the effective imaging area of the

projectile imaging on the infrared imaging sensor, and use the infrared imaging sensor with smaller pixel sizes.

5.2. Experimental analysis

In order to verify the contribution of the projectile radiation energy obtained by the infrared photoelectric tracking system, experiments were carried out at the same detection distance using different projectile sizes, and the captured projectile information is collected. The test conditions are as follows: the illuminance is about 3.0×10^3 cd/m², and the detection distance is 75 m. When the projectile flies at the initial speed of 760 m/s, the system starts to track synchronously. The signal processing module is used to process the captured projectile signal, and the average peak value of the system output projectile signal is shown in Table 1.

Table 1. Projectile signal output by the system at a detection distance of 75 m

No.	Projectile's surface area (cm ²)	Average peak of projectile signal (mV)	Inherent noise signal (mV)
1	1260	2963	402
2	2740	3508	443
3	3120	3825	421
4	3880	4197	416
5	4260	4435	408

It can be seen from Table 1 that when the detection distance is the same, with the increase of the projectile's surface area, the radiation energy of the projectile obtained by the system also increase, while the inherent noise of the system will remain basically unchanged. The experimental results are basically consistent with the theoretical calculation results.

The experiment was carried out at different detection distances and the same size of the projectile, the test results are shown in Table 2. At this time, the projectile's surface area is 4260 cm². It can be seen from Table 2 that when the detection distance increases, the average peak of the projectile signal output by the system has obvious attenuation, which is mainly reflected in the fact that the farther the detection distance, the relative reduction of the radiation area of projectile, resulting in the reduction of the radiation energy received by the infrared imaging sensor, so the average peak of the projectile signal output by the system decreases.

Table 2. Average peak of projectile signal at different detection distances

No.	Detection distance (m)	Average peak of projectile signal (mV)	Inherent noise signal (mV)
1	65	5172	424
2	70	4831	451
3	74	4476	438
4	85	4382	462
5	95	3481	419

Based on the impact of the detection environment on the test results, the experiment is carried out under the same detection distance and different ambient illuminances. The test results are shown in Table 3. At this time, the detection distance is 88 m. It can be seen from Table 3 that with the increase of illuminance, the average peak of the projectile signal output by the system increases slightly, but the amplitude of the increase is not obvious. When the illuminance is about 1.0×10^3 cd/m², the average peak of the projectile signal is about 3249 mV, while when the illuminance is about 4.2×10^3 cd/m², the average peak of the projectile signal is about 3387 mV, the illuminance has increased by three times, and the average peak of the inherent noise has increased by 183 mV, which indicates that in the infrared photoelectric tracking system, the main radiation source is the thermal radiation of the projectile itself, while the environmental illuminance has a relatively small contribution to the thermal radiation of the projectile itself. In addition, when the background illuminance is strong, the external interference increases slightly and the inherent noise increases. Therefore, in order to track the projectile stably under the strong background illuminance, it still needs some improvement.

Table 3. Average peak of projectile signal under the same detection distance and different ambient illuminances

No.	Illuminance (cd/m ²)	Average peak of projectile signal (mV)	Inherent noise signal (mV)
1	1.0×10^3	3249	403
2	1.6×10^3	3818	411
3	2.5×10^3	4265	414
4	3.2×10^3	3476	559
5	4.2×10^3	3387	585

6. Conclusions

According to the detection principle of the infrared photoelectric tracking system, the radiation characteristics of the projectile in the detection area of the system are studied in this paper, the calculation model of the reflected radiation intensity of the projectile under the solar spectrum and surface radiation acting on the projectile's surface, and the calculation model of the infrared radiation

intensity of the projectile itself are established, the total radiation intensity calculation equation of the projectile's surface in the detection area is obtained, and the calculation function of the radiant flux on the infrared imaging sensor of the system is derived; Considering the factors that affect the detection ability of the system, the calculation model of the detection distance of the infrared photoelectric tracking system is constructed, and the corresponding calculation results and test verification are given. From the calculation results and test data, it can be seen that the calculation model proposed in the paper is basically consistent with the test results, but there are certain errors. In the calculation, the ideal conditions are mainly considered, while in the test, in actual environment, the experimental data of the test is slightly less than the theoretical value due to the combined effect of ambient illuminance change, the attenuation of radiation energy incident on optical lens, the atmospheric attenuation and other factors. The theoretical calculation method proposed in this paper can adapt to the detection performance and detection distance calculation of multiple photoelectric sensors in outer ballistic, and provide scientific theoretical support for improving the design of visible light photoelectric detection system and infrared photoelectric detection system.

Acknowledgement

The research content of this paper comes from my research project of the National Natural Science Foundation of China (No. 62001365) and the Key Science and Technology Program of Shaanxi Province (No.2023-YBGY-341).

References

- [1] Fucai Yang, Dedong Yang, Ning Mao, Xueqing Li, *Acta Optica Sinica* **37**(11), 204 (2017).
- [2] Dong Zhao, Huixin Zhou, Hanlin Qin, Kun Qian, Shenghui Rong, Kuanhong Cheng, Shangzhen Song, *Acta Optica Sinica* **38**(2), 46 (2018).
- [3] Cong Tang, Yongshun Ling, Hua Yang, Xing Yang, Wuqin Tong, *Laser and Optoelectronics Progress* **56**(7), 217 (2019).
- [4] Cong Tang, Yongshun Ling, Hua Yang, Xing Yang, Yuan Lu, *Infrared and Laser Engineering* **48**(6), 456 (2019).
- [5] Liu Qiao, Xiaohuan Lu, Zhenyu He, Chunkai Zhang, Wensheng Chen, *Knowledge Based Systems* **34**, 189 (2017).
- [6] Changhao Chen, Xiaoxuan Lu, Bing Wang, Niki Trigoni, Andrew Markham, *IEEE Transactions on Neural Networks and Learning Systems* **32**(12), 5479 (2021).
- [7] Jingxian Liu, Zulin Wang, Mai Xu, *Information Fusion* **53**, 289 (2020).
- [8] Jing Liu, Yongting Deng, Hongwen Li, *Optics and Precision Engineering* **28**(2), 350 (2020).
- [9] Ekstrand Bertil, *Applied Optics* **39**(20), 3495 (2000).
- [10] Qinglian Jia, Yanfeng Qiao, Wenyuan Deng, *Acta Optica Sinica* **29**(4), 937 (2009).
- [11] Weixian Qian, Qian Chen, Guohua Gu, *Infrared and Laser Engineering* **40**(11), 2078 (2011).
- [12] Shiyu Chao, Guixiang Li, Zhihuai Li, Lifeng Yan, *Journal of Air Force Radar Academy* **25**(5), 318 (2011).
- [13] Da Mu, Hongxia Han, *Journal of Changchun University of Science and Technology (Natural Science Edition)* **35**(4), 5 (2012).
- [14] Xia Mao, Le Chang, Weihe Diao, *Journal of Beijing University of Aeronautics and Astronautics* **37**(11), 1429 (2011).
- [15] Jinwei Zhou, Jicheng Li, Zhiguang Shi, Xiaotian Chen, Xiaowei Lu, *Acta Optica Sinica* **35**(5), 62 (2015).
- [16] Qianlin Xing, Huiming Huang, Rensheng Xiong, Tao Yu, *Acta Photonica Sinica* **33**(7), 893 (2004).
- [17] Xiongxiang Wu, Xiaorui Wang, Bingtao Guo, Hang Yuan, Ke Li, Ying Yuan, *Acta Optica Sinica* **38**(4), 291 (2018).
- [18] Cheng Wang, Limin Jiang, Hanyuan Jiang, *Computer Measurement and Control* **29**(6), 136 (2021).
- [19] Yihui Yuan, Junju Zhang, Zuolong Chen, Benkang Chang, *Acta Armamentarii* **31**(8), 1090 (2010).
- [20] Baohui Zhang, Junju Zhang, Benkang Chang, Yihui Yuan, Zuolong Chen, Yunsheng Qian, *Acta Armamentarii* **33**(11), 1319 (2012).
- [21] Hailong, Ao Zhang, Xuemei Liu, Jing Li, Shaoguang Li, *Acta Optica Sinica* **41**(21), 50 (2021).
- [22] Jiahao Xie, Shucai Huang, Daozhi Wei, Zhaoyu Zhang, *Acta Optica Sinica* **42**(18), 85 (2022).
- [23] Qiang Fu, Guangwei Shi, Xin Zhang, *Infrared and Laser Engineering* **42**(8), 1991 (2013).
- [24] Yu Zhong, Xiaoyan Wu, Shucai Huang, Chengjing Li, Hongxia Kang, *Infrared Technology* **36**(7), 582 (2014).

*Corresponding author: xiaoqianzh1983@yeah.net